JOURNAL OF MATERIALS SCIENCE 28 (1993) 6409–6417

Orientation distributions and melting behaviour of extended and folded-chain crystals in gel-drawn, Ultra-high-molecular-weight polyethylene

A. WASIAK, P. SAJKIEWICZ
Laboratory of Polymer Physics, Institute of Fundamental Technological Research, Polish Academy of Sciences, Swietokrzyska 21, 00-049 Warszawa, Poland

X-ray diffraction (XRD) studies on the orientation distributions of the 1 1 0 and 1 0 0 planes in gel-drawn samples of ultra-high-molecular-weight polyethylene (UHMWPE reveal the complex character of the crystal-orientation distribution in the samples. The orientation distribution is composed of two contributions differing in width. The dependence of the contents of both components on the draw ratio, as well as their behaviour during melting of the sample, are studied. The character of the dependencies observed indicate that each component of the orientation distribution can be associated with a separate assembly of crystals occurring in the sample, both having the same orthorhombic crystal structure. The broad component corresponds to only slightly oriented folded-chain crystals, while the narrow component corresponds to almost perfectly oriented extended-chain crystals being composed of stretched macromolecules. The content of the folded-chain crystals decreases with an increase in the draw ratio, whereas the content of the extended-chain crystals increases. During melting, folded-chain crystals melt directly to an amorphous phase, while the extended-chain crystals undergo crystal–crystal transition forming a hexagonal phase.

1. Introduction

The structure of oriented polymers, especially those of very high molecular weight, seems to be composed of several mutually connected elements.

Some features of the structure of such materials seem to be generally accepted, such as the coexistence of structural elements like extended-chain and folded-chain crystals, fibrils, free chains in an amorphous phase, and bounded chains (e.g. tie molecules). The properties of these elements and the interactions between them determine the behaviour of the polymer during such processes as deformation or phase transitions.

Recently Van Aerle and Braam [1], proposed a model describing the structure of oriented polymers. This model is based on an analysis of the structural processes occurring during deformation of the polymer and yielding with the set of elements constituting the structure of the oriented material formed during deformation. The possibility of predicting the dependence of the lateral dimensions of crystals on the draw ratio applied to the sample is one of the consequences of this model. Measurements [1] performed on Ultra-high-molecular-weight polyethylene (UHMWPE) have shown a decrease of the lateral dimensions of crystals at draw ratios below 30, and a slight increase at higher draw ratios. According to [1] these results are consistent with the predictions of the model. It should be mentioned, however, that this result is for data which is an average of the lateral dimensions of all of the types of crystal existing in the system. Consequently, it does not provide separate information on the behaviour of various types of crystals.

Another consequence of this model [1] is the existence of stretched macromolecules, with their ends entrapped in different structural elements (crystals or fibrils). These stretched molecules differ from the other molecules in their crystallization behaviour, being able to form extended-chain crystals.

The presence of extended-chain crystals, composed of stretched molecules, can be associated, in turn, with some peculiarities observed during melting. Several authors [2–9] report the occurrence of a pseudo-hexagonal phase appearing as an intermediate state during the melting of polyethylene under stress or elevated pressure.

As already reported [10, 11] our recent studies on gel-drawn UHMWPE have shown that the crystal-orientation distribution appears to be a superposition of two functions representing broad and narrow contributions. A method of analysing X-ray diffraction (XRD) patterns, permitting the separation of both contributions, was also elaborated [12]. The existence of stronger oriented zones close to zones which were

0022–2461

only weakly oriented or which were unoriented was revealed in drawn UHMWPE by Michler [13] and Matsuo *et al.* [14].

The aim of the present work was to investigate whether or not the existence of the two components of the orientation-distribution function can be associated with the presence of different physical entities in the structure of the material.

The research was carried out by:

(i) studies on lateral crystal sizes separately in each component of the orientation distribution;

(ii) determination of the fractions of both components as functions of the draw ratio applied during preparation of the material, and during stepwise increases of temperature of the sample under constant length; and

(iii) studies on the phase transitions occurring during melting of each component of the orientation distribution.

2. Experimental procedure

2.1. Materials

Drawn foils of UHMWPE Hercules 1900 ($M_w = 3.7 \times 10^3$ kg mol^{-1}) were investigated. Samples were formed using the method described by Smith and Lemstra [15–20].

Four stages in the preparation can be distinguished.

1. A 0.5 wt % solution of Polyethylene (PE) was prepared in decaline (which slightly exceeded the critical concentration [21] required for the formation of a coherent network) by stirring at 150 °C in an atmosphere of nitrogen. Then 0.5 wt % of an antioxidant (N-phenyl-β-naphtylamine) was added to the polymer.

2. The solution was cast to a metal form at 20 °C in order to form a sheet of gel.

3. Polymer foil was precipitated from the gel with methanole; this was followed by drying at room temperature.

4. The foil was drawn at 130 °C in a manually operated stretching device; this was followed by cooling in air to room temperature.

The draw ratio $R = L/L_0$ was determined by measuring the displacement of ink marks, placed 1 mm apart on the specimen surfaces prior to drawing. Up to draw ratios of $R < 2$, the samples showed uniform deformation along their lengths. Further drawing was accompanied by necking resulting in the appearance of highly deformed zones ($R > 2$) in addition to less deformed ($R < 2$) zones. Microscopic observations revealed a fibrillar structure in the highly deformed regions. The structure of highly ($R > 2$) and less deformed parts (usually $R < 2$) of the specimens was further individually characterized.

2.2. Methods of measurement and data evaluation

Wide-angle XRD studies were carried out by means of a flat camera equipped with a temperature chamber and a sample holder permitting the sample to be to kept under constant-length or constant-load conditions [10]. The texture axis was perpendicular to the primary beam, which in.turn was perpendicular to the surface of the photographic film. Nickel-filtered CuK_α radiation was used. Diffraction patterns were registered on Gevaert D7 and D10 films. The sample-to-film distance was chosen as 50 mm, so the 1 1 0 and 2 0 0 reflections of the orthorhombic phase could be simultaneously recorded. Exposure times between 2 and 32 h were chosen to ensure that a large portion of the intensity distribution was located in the linear region of the characteristic curve of the photographic emulsion.

Intensity distributions were measured on X-ray photographs by means of a digital area densitometer [22]. A number of radial intensity distributions, $I_\beta(\theta)$, for different azimuthal angles, β, were obtained. Each intensity distribution was further approximated by the sum of three Pearson VII functions of the form

$$I(\theta) = \frac{I_0}{\{1 + 4[(\theta - \theta_0)/H]^2(2^{1/m} - 1)\}^m} \quad (1)$$

where I_0 is the intensity at maximum, and θ_0 is the position of the maximum of a particular peak, H is its half-width, m is a shape parameter representing the 1 1 0 and 2 0 0 peaks and amorphous halo. The approximation was performed by means of a non-linear optimization program based on a Hook–Jeeves algorithm (cf. [12]). This approach is similar to that presented in [23–26].

The shape of the amorphous halo was assumed not to depend on the deformation and crystallinity nor on the azimuthal angle, β. Consequently, the following parameters of the Pearson VII function were accepted as constants: $\theta_{0,am} = 9.219442°$, $H_{am} = 2.582902°$, $m_{am} = 1.176454$; only the intensity of the halo at its maximum, $I_{0,am}$, was allowed to vary, and it was used as a fitting parameter in the procedure of separating the crystalline peaks. All parameters describing crystalline peaks were, in turn, allowed to vary during optimization. The orientation distributions of the crystallographic-plane normals 1 1 0 and 2 0 0 were determined from the dependence of I_0 for the 1 1 0 and 2 0 0 peaks upon the azimuthal angle, β, further expressed as a function of the orientation angle α, determined by means of the Polany'i equation:

$$\cos\alpha = \cos\theta_0 \cos\beta \quad (2)$$

For each reflection, $h\,k\,l$, the function I_0 was approximated by the following sum of exponential functions (cf. [12]) describing the narrow and broad components of the orientation distribution:

$$I_0(\alpha) = I_1(\alpha)\exp(-A_1^2\cos^2\alpha) + I_2(\alpha)\exp(-A_2^2\cos^2\alpha) \quad (3)$$

The parameters I_n and A_n resulting from the approximation were further used to evaluate the fractions of both contributions, u_n, expressed as

$$u_1 = C_1/(C_1 + C_2), \qquad u_2 = 1 - u_1 \quad (4)$$

where

$$C_n = \int_0^{\pi/2} I_n \exp(-A_n^2 \cos^2\alpha) \sin\alpha \, d\alpha \quad (5)$$

where $n = 1, 2$.

Further, for each crystallographic plane, the orientation factor, f_n, was determined for both components (n) from the equation

$$f_n = \tfrac{1}{2}(3\langle\cos^2\alpha\rangle - 1) \quad (6)$$

where

$$\langle\cos^2\alpha\rangle = \frac{\int_0^{\pi/2} I_n \exp(-A_i^2 \cos^2\alpha) \cos^2\alpha \sin\alpha \, d\alpha}{\int_0^{\pi/2} I_n \exp(-A_n^2 \cos^2\alpha) \sin\alpha \, d\alpha} \quad (7)$$

The lateral dimensions of the crystals were determined from the half-widths of the 1 1 0 and 2 0 0 lines measured from azimuthal scans at various β-angles. Broadening of the diffraction lines was assumed to be only dependent on the crystal size, while the effects of distortions were neglected.

Since *changes* of crystal size were of interest rather than their absolute values, only the relative dimensions were computed, as follows

$$D_{rel} = \frac{D}{D_{ref}} = \frac{H_{ref}}{H} \quad (8)$$

An undrawn PE sample, annealed under vacuum for 100 h at 130 °C, was used as a reference. The following values were obtained for H_{ref}: 0.28° for the line 1 1 0, and 0.34° for the line 2 0 0.

At azimuthal angles where broad and narrow components of the orientation distribution overlapped, the corresponding profiles were separated by subtraction of the profile corresponding to the broad component from the measured profile. The profile to be subtracted was determined in such a way that the parameters m, H and α of the Pearson VII function at the desired angle were accepted as being equal to those determined at an azimuthal angle where only the broad component existed; so they are assumed to be independent of the orientation angle. The intensity at maximum for the broad component at the desired orientation angle, α, was determined from the corresponding part of Equation 3.

The studies at elevated temperatures concerned identification of the phases occurring during the melting of each component of the orientation distribution. Three types of samples were used. The first ($R = 1.5$) contained only the broad component of the orientation distribution, the second ($R = 30$) contained only the narrow component, while the third ($R = 6$) contained contributions of both components (broad and narrow).

Melting experiments were performed by a stepwise increase of the temperature of the sample at a constant length. At each step, the temperature was held constant for the time required for an XRD photograph. Some time (approximately 15 min) was allowed for stabilization of the structure at a given temperature prior to X-ray exposure.

The following relative measures of the contents of the amorphous and hexagonal phases were defined and experimentally evaluated:

$$\kappa = \frac{\int_0^{\pi/2} I_0(\alpha) \sin\alpha \, d\alpha}{\int_0^{\pi/2} I_{0\,(max)}(\alpha) \sin\alpha \, d\alpha} \quad (9)$$

where $I_0(\alpha)$ denotes the intensities scattered in amorphous regions or on the 1 0 0 plane of the hexagonal phase, measured at a given temperature, while $I_{0,max}(\alpha)$ denotes the corresponding intensities at the temperature at which the intensity of a particular form (amorphous or hexagonal) reached a maximum.

3. Results

3.1. Studies at room temperature

Fig. 1 shows XRD photographs illustrating the structure of UHMWPE samples drawn at various draw ratios, R. As can be seen, at small deformations ($R \sim 1.5$) only broad distributions of orientations can be distinguished. Indeed, in those cases, the azimuthal intensity distribution is approximated by only one term from Equation 3. At higher draw ratios, where the fibrillar structure of the material can be recognized, another component having a narrow distribution is visible in addition to the broad distribution of orientations. The approximation, shown in Fig. 2, of the intensity distribution evidently yields with Equation 4 two non-zero values of the fractions of both components. An increase in the deformation leads to a decrease in the fraction of the broad component. Consequently, above some value of the draw ratio, only the narrow component is visible (cf. Fig. 1e). The dependencies of the fractions, u_n, and of the orientation factors, f_n, upon the draw ratio, R, for both components (broad and narrow) of the orientation distribution are shown in Fig. 3.

The fraction, u_1, of the broad component, initially equal to unity at very low draw ratios, further decreases with an increase of the draw ratio, R. The decrease of the content of the broad component is accompanied by an increase of the fraction of the narrow component, appearing above draw ratios of $R = 2$. At a draw ratio of $R = 30$, the fraction, u_2, of the narrow component practically reaches unity.

The orientation factor of the broad component varies from 0 to almost perfection ($f_1 \sim -0.5$), indicating a gradual increase of orientation with increasing draw ratio. In the case of the narrow component of the orientation distribution, its orientation is nearly perfect ($f_2 \sim -0.5$) even at relatively small draw ratios. An increase of the draw ratio leads to only a slight further increase of the orientation factor (asymptotically approaching -0.5).

Broadening of the 1 1 0 and the 2 0 0 diffraction lines, when determined separately for each component of the orientation distribution, clearly indicates that the sizes of the crystals constituting each component

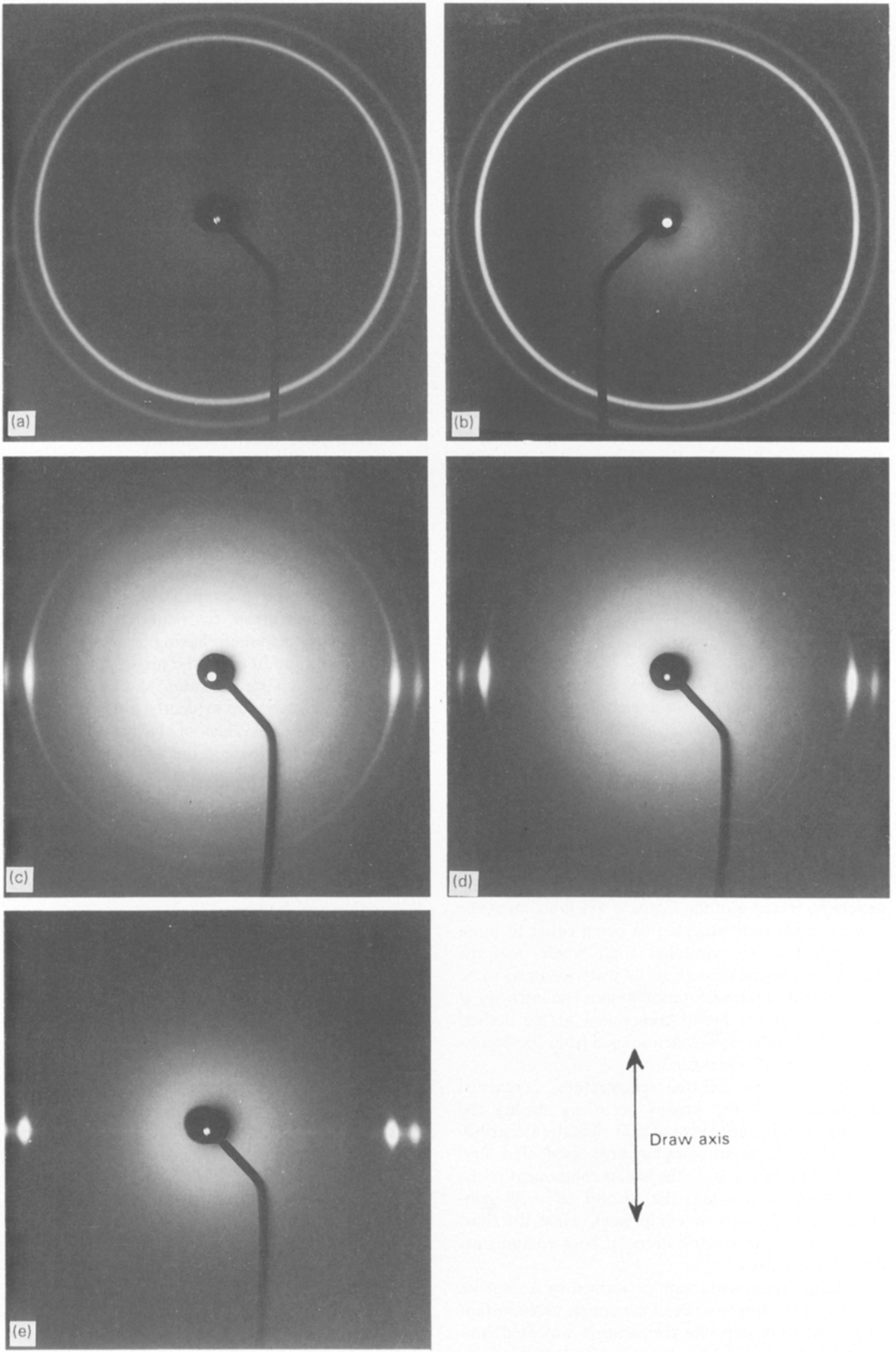

Figure 1 XRD patterns obtained from samples drawn to various draw ratios: (a) $R = 1$, (b) $R = 1.5$, (c) $R = 6$, (d) $R = 14$, and (e) $R = 30$.

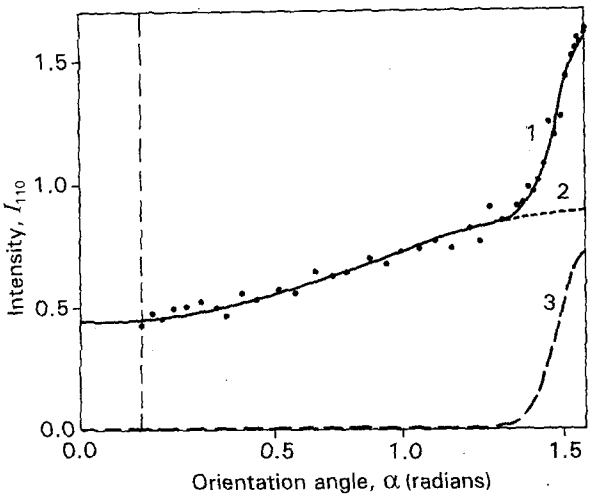

Figure 2 Separation of the broad (curve 2) and narrow (curve 3) components of the azimuthal intensity distributions $I_0(\alpha)$ (curve 1) for the line 1 1 0 in the sample drawn to $R = 6$.

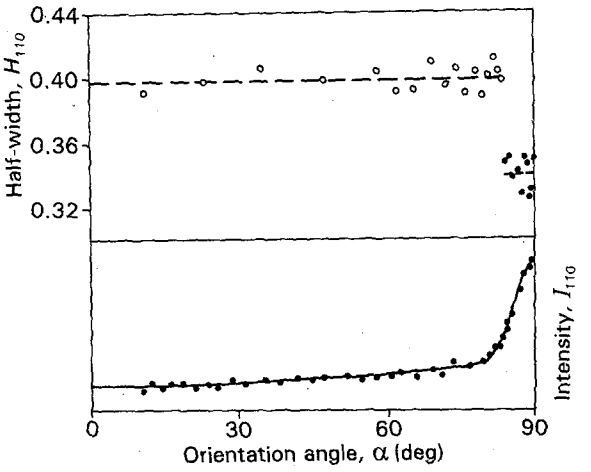

Figure 4 Comparison of the orientation dependencies of (——) the intensity, I_0, and (– – –) the half-width, H, for the 1 1 0 line of the sample drawn to $R = 6$.

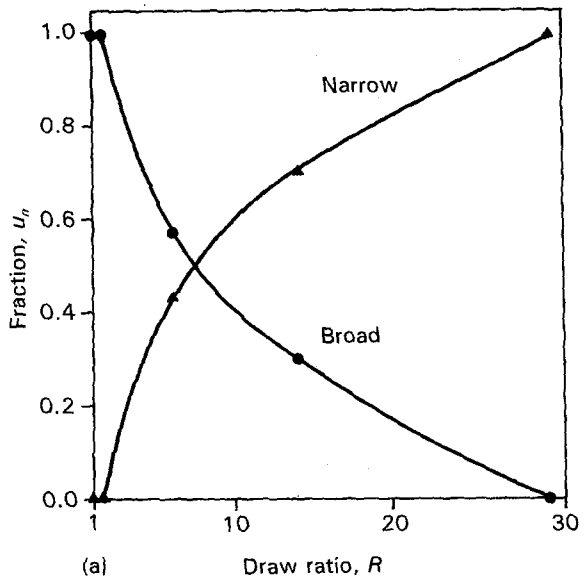

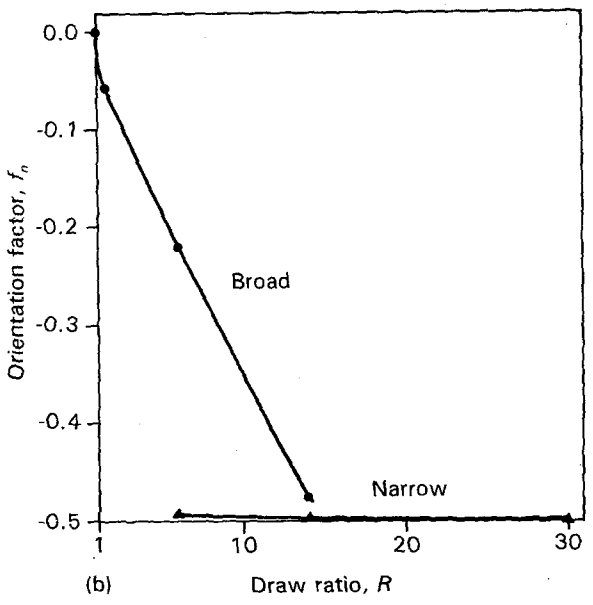

Figure 3 (a) Changes of the fractions, u_n, and (b) the orientation factors, f_n, of the broad and narrow components of the orientation distribution. The dependencies are characteristic of both the 1 1 0 and 2 0 0 planes.

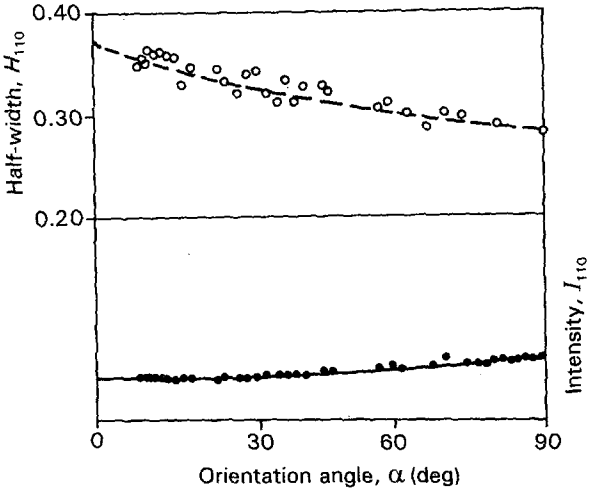

Figure 5 Comparison of the orientation dependencies of (——) the intensity, I_0, and (– – –) the half-width, H, for the 1 1 0 line of the sample drawn to $R = 1.5$.

are different. Fig. 4 shows the dependencies upon the orientation angle, α, of the intensity at maximum, $I_{0,1\,1\,0}$, and half-width, $H_{1\,1\,0}$, determined for a draw ratio of $R = 6$, that is, for the sample containing both components. As can be seen, the line width (crystal size) is practically independent of the orientation angle within each component of the orientation distribution. Only at very low draw ratios, when only the broad component existed, was a small dependence of H upon the orientation angle detected. This dependence is shown in Fig. 5. It can be seen in Fig. 5 that the better oriented the crystal is, the larger is its size. It might indicate, that low deformation, which does not lead to the appearance of crystals constituting the narrow component, more effectively orients bigger crystals than small ones, or that crystals with their 1 1 0 or 2 0 0 directions perfectly oriented with respect to the direction of drawing might undergo some scission processes, while the size of those crystals perpendicular to the direction of drawing remains unchanged.

At a draw ratio of $R = 14$, the width of the 1 1 0 line corresponding to the narrow component is smaller (a bigger crystal size) than that of the broad component.

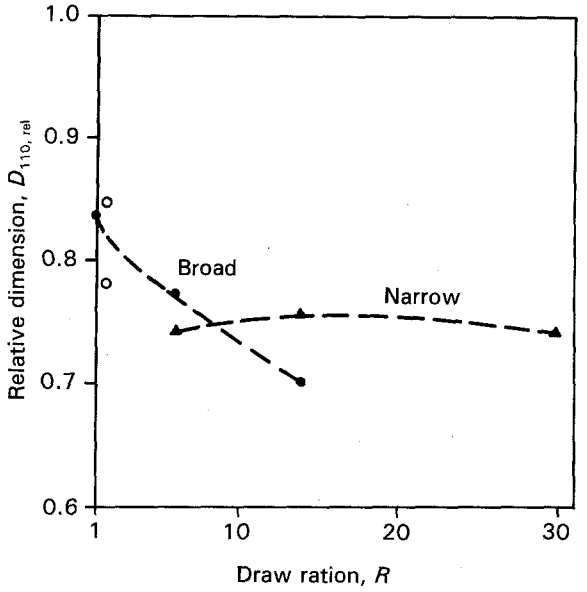

Figure 6 Relative lateral sizes of the crystals in the narrow and broad components measured from 1 1 0 line broadening as a function of the draw ratio, R. (○) The points at $R = 1.5$ were calculated from the highest and lowest value of the dependence of the half-width upon the orientation angle shown in Fig. 5.

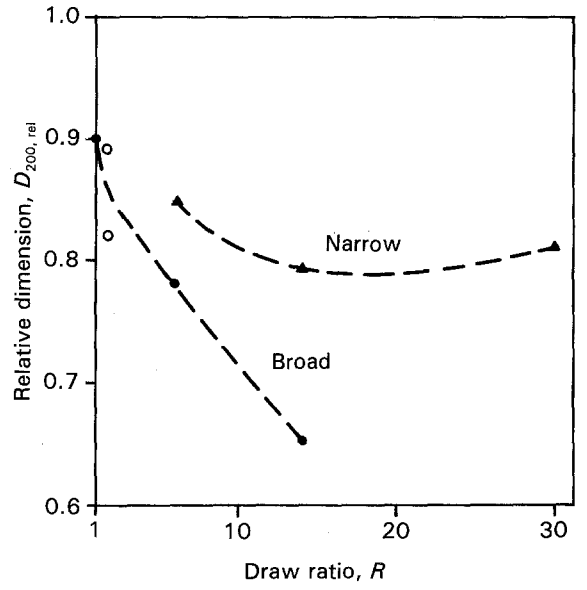

Figure 7 The relative lateral sizes of the crystals in the narrow and broad components measured from 2 0 0 line broadening as a function of the draw ratio, R. (○) The points at $R = 1.5$ were calculated from the highest and lowest value of the dependence of the half-width upon the orientation angle.

An inverse relation between the lateral sizes of the crystals constituting both components of the orientation distributions can be observed for the 1 1 0 line at draw ratios lower than $R \approx 8$ (Fig. 6).

The dependence of the lateral crystal sizes in the direction perpendicular to the 2 0 0 planes upon the draw ratio, R, for both the components of the orientation distributions is shown in Fig. 7.

Figs 6 and 7 demonstrate that, in the case of the broad component of the orientation distribution, an increase of the draw ratio leads to a decrease of the lateral crystal sizes. On the contrary, the lateral sizes of the crystals constituting the narrow component do not change substantially with the draw ratio. The dependencies of the crystal size upon the draw ratio are, however, somewhat different for the narrow and broad components, as well as for the 1 1 0 and 2 0 0 planes. The dependence of the lateral crystal sizes upon the draw ratio for the broad component resembles, in a qualitative way, the initial part of the dependence observed by van Aerle and Braam [1] for UHMWPE samples formed from a 2% solution. In this case, however, only one component of the orientation distribution was detected.

3.2. Melting

A peculiar melting behaviour was observed when drawn samples of UHMWPE were heated at constant length. In some cases orthorhombic crystals melted, yielding an amorphous melt directly, while in other cases an intermediate hexagonal phase was formed at some temperature. The presence of this phase is indicated by an additional diffraction line appearing at elevated temperatures at $2\theta = 20.46°$. XRD photographs showing the subsequent stages of melting in the situation when the hexagonal phase had formed are presented in Fig. 8. It is evident that the melting behaviour of the sample is determined by the draw ratio, and also by the presence of the broad and narrow components of the orientation distribution.

Samples drawn to small draw ratios, in which only the broad component was present, melted directly to an amorphous phase.

In contrast, highly drawn samples, containing only the narrow component, transformed completely into a hexagonal phase, which melted to an amorphous one phase: upon further heating. In such samples, a constant fraction of the amorphous phases was observed until transformation of the orthorhombic phase into the hexagonal phase was complete.

The most complicated situation was observed in samples drawn to intermediate draw ratios, containing both the narrow and broad components. In such cases two processes occur simultaneously: direct melting of orthorhombic crystals into an amorphous melt, and crystal–crystal transition from orthorhombic to hexagonal crystals. As shown in Fig. 9, the amorphous intensity is observed to increase with increases in the temperature, for temperatures lower than 145 °C – when the hexagonal phase appeared. It has to be pointed out that the increase in the amorphous intensity stopped at the same temperature at which the broad component completely disappeared. Above this temperature the content of the narrow component decreased and was accompanied by an increase in the content of the hexagonal phase, while the content of the amorphous phase remained constant. The maximum content of the hexagonal form coincided with complete disappearance of the orthorhombic crystals. A further increase in the temperature caused a decrease in the content of the hexagonal crystals, and again an increase in the content of the amorphous phase.

This pattern of changes clearly indicated that orthorhombic crystals constituting the narrow component of the orientation distribution transfomed upon

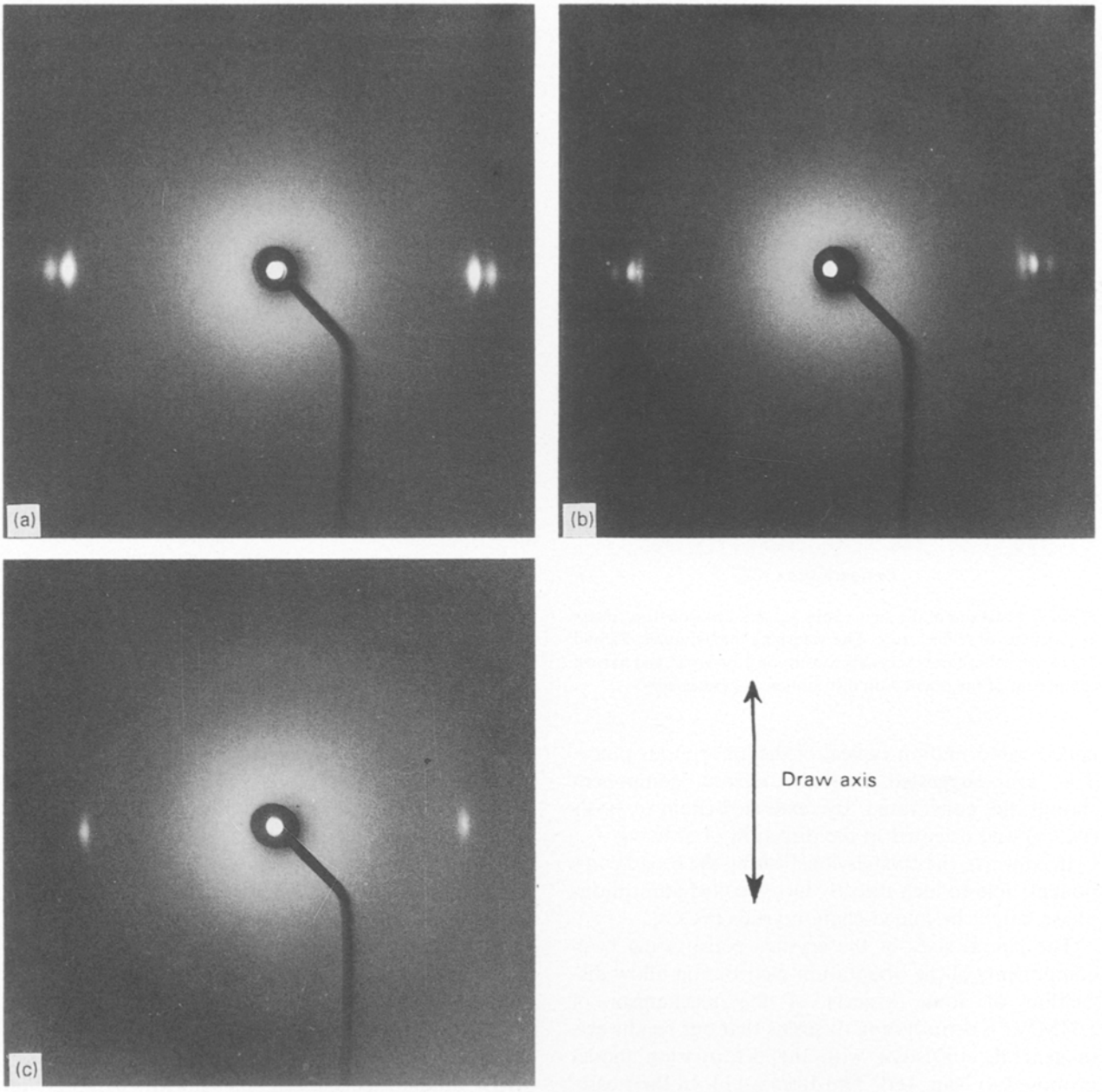

Figure 8 XRD photographs taken on the subsequent stages of melting of the sample kept under constant length. (a) $T = 20\,°C$, the 1 1 0 and 2 0 0 lines of the orthorhombic phase are visible. (b) $T = 147.4\,°C$, the 1 1 0 and 2 0 0 lines of the orthorhombic phase and a line of the hexagonal phase are visible. (c) $T = 149.5\,°C$, only the line of the hexagonal phase remains.

heating into a hexagonal form, while the orthorhombic crystals remaining in the broad component melted directly to an amorphous phase.

Hexagonal crystals also directly formed an amorphous melt during their fusion. The final temperature, at which the hexagonal phase disappeared was not been reached in the present work. At 155.3 °C, the highest temperature at which the system was investigated, the difraction line of the hexagonal phase was still present. This is consistent with some literature data [27] indicating that the melting temperature of this phase might be as high as 180 °C.

The azimuthal intensity distribution of the amorphous halo showed no angular dependence. The line 1 0 0 of the hexagonal phase showed, in turn, well pronounced azimuthal dependence. In contrast to the orthorhombic crystals, the orientation distribution of the hexagonal crystals was composed of only one component. It was slightly broader than the distribution of the orthorhombic crystals observed at the same temperature. The maximum of the intensity distribution of the hexagonal line was located on the equator of the X-ray diagram, which indicated that macromolecules were parallel to the direction of drawing.

3.3. Discussion

The differences observed in the melting behaviours of both the broad and narrow components of the orientation distribution allow the conclusion that the crystals constituting the narrow component of the orientation distribution are formed from constrained molecules. Since melting of those crystals leads to a well-oriented hexagonal phase it seems that they are formed from extended chains under tension, which prevents them from assuming, during melting, the

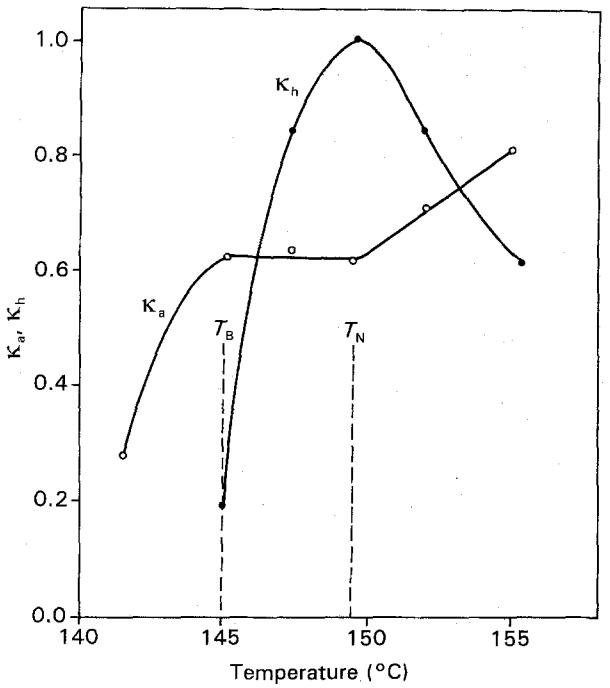

Figure 9 Fractions of the amorphous, κ_a, and hexagonal, κ_h, phase as functions of temperature. The vanishing temperatures, T_B and T_N, of the orthorhombic crystals constituting the broad and narrow component of the orientation distribution are indicated.

coiled conformation typical of the amorphous phase. This also suggested that the narrow component should be constituted by extended-chain crystals (ECCs) well oriented in the direction of drawing.

In contrast, the crystals constituting the broad component, able to melt directly into a coiled amorphous phase, might be folded-chain crystals (FCCs).

The lateral sizes of the crystals constituting both components of the orientation distribution allow discussion of some aspects of the mechanism of UHMWPE deformation. It seems that our results are, in general, consistent with the deformation model proposed by van Aerle and Braam [1]. In their case, however, only one component of the orientation distribution was detected, and therefore the measured crystal sizes were average values of the lateral dimensions of the FCCs and ECCs while in our case both types of crystals were distinguished and separately characterized. At low draw ratios, $R < 2$, the FCCs were slightly oriented with their c-axis in the drawing direction. The azimuthal distributions of the lateral crystal sizes indicated that either bigger crystals orient themselves more effectively than small ones, or that crystals which are perfectly oriented with respect to the direction of drawing prior to deformation do not undergo any scission. Consequently, the size of perfectly oriented crystals remains unchanged while the other crystals underwent fragmentation during drawing. At higher deformations, the chains (which effectively transmitted the drawing force) straightened forming ECCs with a narrow orientation distribution. The process of formation of ECCs is accompanied by a decrease in the content and lateral sizes of FCCs. This observation is consistent with a deformation mechanism by fragmentation of FCCs, as proposed by van Aerle and Braam [1].

An increase in the content of the narrow component with an increase in the draw ratio can also be explained on the basis of this model [1]. The occurrence of the narrow component was, in the present work, observed at draw ratios as low as about $R = 2$. Since, in our opinion, the narrow component that always melts by transition to a hexagonal phase consists of ECCs which are almost perfectly oriented along the drawing direction. Existence of these crystals (ECCs), undoubtedly formed from constrained and elongated macromolecules, at such low draw ratios cannot therefore be explained on the basis of the above model [1]. Some other mechanism of structure formation should be adopted. Since the orientation of the hexagonal phase does not relax after orthorhombic crystals completely melt, it might be considered that lamellar crystals are not the only possible constraints that keep some of the chains extended. Chain entanglements that should exist after the crystals are molten might play a similar role. Since the number of entanglements occurring in the system is drastically reduced by the gel-drawing procedure, it is quite possible that ECCs constituting the narrow component of the orientation distribution are formed by macromolecules which survived in an entangled form through the gel stage of preparation. An important role of the entanglements between crystal lamellae for transmitting the drawing force in an ultradrawing process may be concluded from the results obtained by Matsuo *et al.* [14]; they investigated UHMWPE samples with a molecular weight of 6×10^6, cast from solution with a critical concentration of 0.4 g per 100 ml. The results [14] reveal, in the drawn specimens, the coexistence of oriented and unoriented zones. They have shown that an increase in the number of entanglements causes a decrease in the content of the unoriented regions.

4. Conclusions

XRD studies performed on drawn samples of UHMWPE, both at room temperature and during a gradual increase in the temperature up to melting, revealed the following features of the investigated material.

1. Only the samples drawn to draw ratios of $R < 2$ were deformed uniformly along the sample length and they contained crystals with a relatively broad orientation distribution. Further drawing was accompanied by necking resulting in relatively highly deformed zones ($R > 2$) containing two types of crystals composing the broad and narrow components of the orientation distribution.

2. The fraction of each component, and the degree of orientation of the broad component, depended upon the draw ratio, R, while the very high degree of orientation of the narrow component appeared to be almost independent of R.

3. Crystals constituting the broad component, able to melt directly into a coiled amorphous phase, might be the folded-chain lamellar crystals.

4. Crystals constituting the narrow component are formed from elongated and constrained macromolecules. These crystals, were probably extended-

chain crystals which, prior to melting, underwent crystal –crystal transition into a well-oriented hexagonal phase that finally melted above 155 °C. The nature of the constraints holding the macromolecules in a stretched state is not completely understood. They might be mainly due to chain entanglements; but, especially in the early stages of melting, some role might also be played by entrapment of parts of the macromolecules into different crystals.

References

1. N. A. J. M. VAN AERLE and A. W. M. BRAAM, *J. Mater. Sci.* **23** (1988) 4429.
2. S. B. CLOUGH, *J. Appl. Polym. Sci.* **15** (1971) 2141.
3. J. SMOOK and A. J. PENNINGS, *Coll. Polym. Sci.* **262** (1984) 712.
4. M. YASUNIWA, R. ENOSHITA and T. TAKEMURA, *Jpn. J. Appl. Phys.* **15** (1976) 1421.
5. D. C. BASSET, S. BLOCK and G. PIERMARINI, *J. Appl. Phys.* **45** (1974) 4146.
6. G. UNGAR and A. KELLER, *Polymer* **21** (1980) 1273.
7. A. J. PENNINGS and A. ZWIJNENBURG, *J. Polym. Sci., Polym. Phys. Ed.* **17** (1979) 1011.
8. T. ASAHI, *ibid.* **22** (1984) 175.
9. M. YASUNIWA and T. TAKEMURA, *Polymer* **15** (1974) 661.
10. P. SAJKIEWICZ, *IFTR Reports* **12** (1990).
11. P. SAJKIEWICZ and A. WASIAK, in Proceedings of the 19th Europhysics Conference on Macromolecular Physics, Gargnano, Italy, June 1988, p. 99.
12. *Idem. J. Appl. Cryst.* **23** (1990) 88.
13. G. H. MICHLER, *Coll. Polym. Sci.* **270** (1992) 627.
14. M. MATSUO, C. SAWATARI, M. IIDA and M. YONEDA, *Polym. J.* **17** (1985) 1197.
15. P. SMITH, P. J. LEMSTRA, J. P. L. PIJPERS and A. M. KIEL, *Coll. Polym. Sci.* **259** (1981) 1070.
16. P. SMITH, P. J. LEMSTRA, *J. Mater. Sci.* **15** (1980) 505.
17. P. SMITH, P. J. LEMSTRA, B. KALB and A. J. PENNINGS, *Polym. Bull.* **1** (1979) 733.
18. P. SMITH and P. J. LEMSTRA, *Makromol. Chem.* **180** (1979) 2983.
19. *Idem. Coll. Polym. Sci.* **258** (1980) 891.
20. P. SMITH, P. J. LEMSTRA and H. C. BOOIJ, *J. Polym. Sci. Polym. Phys. Ed.* **19** (1981) 877.
21. P. SAJKIEWICZ, *Polimery* **36** (1991) 245.
22. M. KOSC and A. WASIAK, *IFTR Reports* **33** (1988).
23. H. M. HEUVEL, R. HUISMAN and K. C. LIND, *J. Polym. Sci., Polym. Phys. Ed.* **14** (1976) 921.
24. H. M. HEUVEL and R. HUISMAN, *ibid.* **19** (1981) 121.
25. D. P. ANDERSON, X-ray Analysis Software: Operation and Theory involved in the Program "Diff". Interim Report for the Period May 84 to March 85, University of Dayton Research Institute (1985).
26. R. SCIGALA, A. WLOCHOWICZ, *Acta Polymerica* **40** (1989) 15.
27. A. E. ZACHARIADES and J. A. LOGAN, *J. Polym. Sci., Polym. Phys. Ed.* **21** (1983) 821.

Received 23 November 1992
and accepted 24 May 1993